



Supported Co/activated carbon catalysts for the one-pot synthesis of isophorone diamine from hydroamination of isophorone nitrile

Zuojun Wei¹ · Haiyan Liu¹ · Kuo Zhou² · Huimin Shu² · Yingxin Liu²

Received: 18 March 2019 / Accepted: 27 May 2019 / Published online: 4 June 2019
© Akadémiai Kiadó, Budapest, Hungary 2019

Abstract

Supported Co/activated carbon (Co/AC) catalysts were prepared by the incipient wetness impregnation method and applied to the one-pot hydroamination of isophorone nitrile (IPN) into isophorone diamine (IPDA). The 20 wt% Co/AC heat-treated in N₂ exhibited superior catalytic performance to the 20 wt% Co/AC heat-treated in H₂, by which a maximum 90.2% yield of IPDA was achieved and it could be recycled at least four times. XRD, XPS, TEM and BET has demonstrated that the existence of the fcc form of Co as well as the smaller and more uniformly dispersed Co particles in the Co/AC catalyst heat-treated in N₂ may contribute to the excellent catalytic performance.

Keywords Carbon reduction · Co/AC · Hydroamination · Isophorone diamine · Isophorone nitrile

Introduction

Isophorone diamine (IPDA) is an important alicyclic amine derived from the downstream products of acetone. Because of its unique amino structure, IPDA is widely used as a solidifying agent for epoxy resins, showing excellent stain resistance, oil resistance, weatherability, color stability, low viscosity, and shrinkage [1]. It is also

Electronic supplementary material The online version of this article (<https://doi.org/10.1007/s11144-019-01606-9>) contains supplementary material, which is available to authorized users.

✉ Yingxin Liu
yxliu@zjut.edu.cn

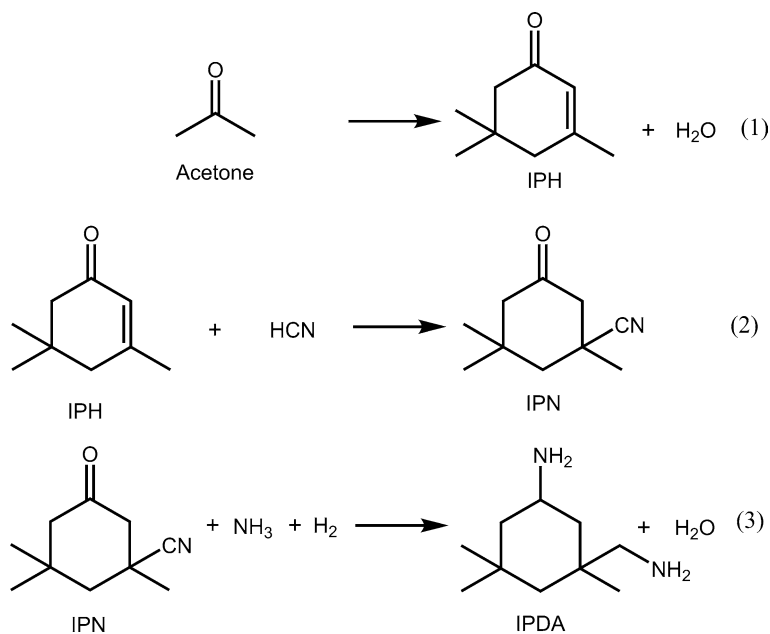
¹ Key Laboratory of Biomass Chemical Engineering of the Ministry of Education, College of Chemical and Biological Engineering, Zhejiang University, 38 Zheda Road, Xihu District, Hangzhou 310027, People's Republic of China

² Research and Development Base of Catalytic Hydrogenation, College of Pharmaceutical Science, Zhejiang University of Technology, 18 Chaowang Road, Xiacheng District, Hangzhou 310014, People's Republic of China

a raw material to isophorone diisocyanate, which is another popular material in the fields of polyurethane and paint [2]. IPDA can be synthesized through the following pathway (Scheme 1): firstly, isophorone is obtained by cyclocondensation of three molecules of acetone [3, 4], followed by the cyanation of isophorone to obtain isophorone nitrile (IPN) [5, 6]; finally, IPDA is obtained by hydroamination of IPN [7].

The hydroamination of IPN proceeds in two steps, the iminization of the carbonyl group and the subsequent hydrogenation of imine and cyano groups [8, 9]. Generally, the iminization of the carbonyl group is catalyzed by an acid or base catalyst [10], whereas it can also occur spontaneously without any catalyst [11]. However, metal hydrogenation catalysts (e.g., Ni, Co, Ru) are essential to hydrogenation reaction of imine and cyano groups [12, 13]. For example, in the hydroamination of carbonyl groups, Chatterjee et al. [14] applied Rh/Al₂O₃ to hydroamination of furfural into furfurylamine, in which the support Al₂O₃ may serve as a dual acid/base catalyst for iminization of carbonyl. While Christian et al. [15] only used Raney Ni for hydroamination of cyclohexanone to cyclohexylamine. In the hydrogenation of the cyano group, Segobia et al. [16] used Ni/SiO₂ for the hydrogenation of *n*-butyronitrile to *n*-butylamine McAllister et al. [17] utilized Pd/C to catalyze the hydrogenation of 4-hydroxybenzyl cyanide to primary amine tyramine.

In our previous work, CaO plus Raney Co and Co/SiO₂ were used for the hydroamination of IPN achieving 95.6 mol% and 70.4 mol% yield of IPDA, respectively [18, 19]. Nevertheless, Raney Co is criticized for easy inactivation, high dosage and weak mechanical strength, which limits its industrial application [20, 21]. In order to further improve the yield of IPDA over a supported Co-based catalyst



Scheme 1 Pathway of synthesis of IPDA from acetone

for future industrial use, herein, we continued to screen the commercially available supports and found that Co/AC catalysts performs the best in hydroamination of IPN into IPDA. Meanwhile, the XRD, BET, XPS and TEM of the Co/AC catalysts were characterized to disclose its structure–function relationship.

Experimental section

Materials

IPN was synthesized in our laboratory with a purity of more than 98.5%. Raney Co was purchased from Shanghai Sun Chemical Technology Co. Ltd. Ammonia, hydrogen and nitrogen gases were provided by Hangzhou Jin gong Special Gas Co. Ltd., with purity larger than 99.99%. Other chemicals are analytical reagents and were purchased from Sino-pharm Chemical Reagent Co. Ltd.

Catalyst preparation

The supported Co/active carbon (Co/AC) catalysts were prepared by the incipient-wetness impregnation method. Taking 20 wt% Co/AC catalyst as an example, the typical preparation steps were as follows: 3 g of AC was impregnated with an aqueous solution of $\text{Co}(\text{NO}_3)_2 \cdot 6\text{H}_2\text{O}$ (3.7 g of $\text{Co}(\text{NO}_3)_2 \cdot 6\text{H}_2\text{O}$ dissolved in 6.3 g of H_2O) at room temperature and maintained overnight. The mixture was dried at 110 °C in a vacuum oven for 10 h to form the Co/AC precursor. The precursor was heat-treated at 500 °C in N_2 and H_2 for 4 h. The formed catalysts were denoted as Co/AC (N_2) and Co/AC (H_2) accordingly.

Catalyst characterization

XRD, TEM, BET and XPS characterizations are similar to our previous publications [22, 23] and therefore included in the supporting materials for duplicate-checking reasons.

IPN preparation

The 10 g (0.0669 mol) IPH, 2.0 g (0.0408 mol) NaCN and 9 mL (0.116 mol) *N,N*-dimethyl formamide (DMF) were added into a three-necked round-bottom flasks and heated to 120 °C under continuous stirring. Successively, 5 mL of NH_4Cl (6 mol L^{-1}) was dropwise added into the above mixture and the reaction was maintained for 4 h. A gas chromatography was used to detect the IPN yield (based on NaCN). The reaction mixture was separated by decompressing distillation process and the fraction of 180–200 °C was collected, followed by cooling and recrystallization. Finally, white crystal with 98.5% purity was obtained.

Melting point: 65–66 °C; FT-IR(KBr, cm^{-1}): 3000–2850($\nu\text{C-H}$), 2240–2222($\nu\text{C}\equiv\text{N}$), 1715($\nu\text{C=O}$), 1465 ~ 1340($\delta\text{C-H}$); $^1\text{H-NMR}$ (500 MHz,

CDCl_3): δ = 2.69 (dt, J = 14.3, 1.9 Hz, 1H), 2.30–2.15 (m, 3H), 2.12–2.04 (m, 1H), 1.66 (dd, J = 16.0, 9.4 Hz, 1H), 1.52 (s, 3H), 1.21 (s, 3H), 1.10 (s, 3H); MS (EI, 70 eV) m/z (%): 165 (M^+ , 13), 150 (10), 94 (17), 83 (100).

Catalytic reaction

The iminization and one-pot hydroamination reactions were carried out in the same 100 mL stainless steel autoclave equipped with a mechanical stirrer. 40 mL of methanol (solvent), 2.5 g of IPN, and 0.5 g of Co-based catalysts were introduced into the reactor. After the reactor was sealed and purged with N_2 to remove air, ammonia was introduced up to 0.2 MPa and then hydrogen was introduced up to 8.0 MPa with continuous stirring at 1500 rpm to initiate the reaction for 8 h.

Product analysis

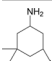
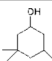
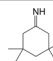
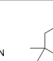
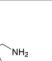
The product analysis section is the same as that in our previous publications [19] and therefore included in the supporting materials for duplicate-checking reasons. The conversion and yield were used to evaluate the transformation of the substrate and the distribution of the products (conversion = $(1 - \text{final amount of IPN}/\text{initial amount of IPN}) \times 100\%$; yield = $(\text{mole amount of each product}/\text{mole amount of initial IPN}) \times 100\%$).

Results and discussion

Effect of the supports

The commercially available chemicals, i.e., NaZSM-5, CaO, γ - Al_2O_3 , AC, SiO_2 and TiO_2 were chosen as support for Co by the incipient-wetness impregnation method for hydroamination of IPN into IPDA. The Raney Co was used as a control group. As illustrated in Table 1, IPN is 100% converted in each entry, regardless of the alkalinity or acidity of the support, indicating that the iminization step may easily occur without any catalyst. Whereas, the catalysts show great difference in the yield of IPDA, among which Co/NaZSM-5 and Co/CaO display inferior yield to IPDA of less than 10 mol% (entries 1 and 2). This should be ascribed that NaZSM-5 has very small pore size of around 0.5 nm and CaO is almost nonporous, which is unfavorable for dispersion of Co into nano size [24, 25]. As a consequence, these two catalysts exhibit poor hydrogenation effect so that a lot of iminization intermediates co-exist in the final product. Besides, the strong alkalinity of the support may inhibit the reduction of Co catalyst precursor, [26–28] resulting in poor hydrogenation ability of the catalysts and the decomposition of IPN to isophorone, as evidenced by the considerable amount of 3, 3,5-trimethyl cyclohexylamine in the product. Among the tested catalysts, Co/AC shows the best catalytic performance with yield to IPDA of 79.7 mol%. Co/ SiO_2 ranks second with 69.0 mol% yield to IPDA. While Co/ TiO_2 and Co/ γ - Al_2O_3 come next with approximately 20 mol% yield to IPDA and a plenty

Table 1 Performance of different catalysts

Entry	Catalyst	Conversion (%)	Yield (%)					Others
								
1	Co/NaZSM-5	100	22.3	–	46.9	8.9	3.2	18.7
2	Co/CaO	100	19.1	–	52.1	3.5	0.2	25.1
3	Co/Al ₂ O ₃	100	11.5	2.3	23.4	20.1	7.9	34.8
4	Co/AC (N ₂)	100	7.4	1.1	7.0	79.7	–	4.8
5	Co/SiO ₂	100	1.5	4.1	10.3	69.0	12.4	2.7
6	Co/TiO ₂	100	–	–	32.5	26.1	27.6	13.8
7 ^a	Raney Co	100	4.9	3.9	1.6	80.4	2.3	6.9

Reaction conditions: IPN, 2.5 g; methanol, 40 mL; NH₃ pressure, 0.2 MPa; H₂ pressure, 8 MPa; supported Co catalyst with loading amount of 20 wt%, 1.0 g; temperature, 80 °C; reaction time, 8 h; stirring speed, 1500 rpm

^a1.3 g of Raney Co

of 3-aminomethyl-3, 3,5-trimethyl cyclohexanol and other unknown substances are produced in the reaction. We therefore consider that AC is preferred as the support under the applied conditions.

It is noted that 1.3 g Raney Co achieved 80 mol% yield of IPDA (entry 7), which is comparable to 20 wt% Co/AC (N₂) of 1.0 g. Bearing in mind that Co metal dosage in Raney Co is six times higher than that of Co/AC (N₂), we consider the latter has strikingly improved metal utilization.

Catalytic performance and recyclability of Co/AC

Further optimization on reaction conditions for Co/AC (N₂) shows that the heat-treatment temperature, catalyst dosage and loading affect the catalytic performance remarkably (Table 2 and Tables S1–S4). A higher catalyst dosage seems essential to the reaction. This is mainly because that NH₃ is more strongly adsorbed on the active sites of the Co surface than H₂, which decreases the hydrogenation activity of the catalyst, as proved by our previous DFT calculation [29]. However, when the dosage is larger than 1.0 g, the yield of IPDA increases slower, and the increase

Table 2 Performance of Co/AC catalysts for IPN hydroamination to IPDA

Entry	Catalysts	Heat-treatment temperature (°C)	Loading (wt%)	Dosage (g)	Conversion (%)	Yield (%)
1	Co/AC (N ₂)	500	20	1.3	100	81.1
2	Co/AC (N ₂)	500	20	2.5	100	90.2
3	Co/AC (H ₂)	500	20	1.3	100	67.4

Reaction conditions: IPN, 2.5 g; methanol, 40 mL; NH₃ pressure, 0.2 MPa; H₂ pressure, 8 MPa; temperature, 80 °C; reaction time, 8 h; stirring speed, 1500 rpm

of IPDA yield may be limited while the dosage of catalyst is higher than 2.5 g, at which a highest IPDA yield of 90.2 mol% is achieved at 500 °C for catalyst heat-treatment and 20 wt% for catalyst loading.

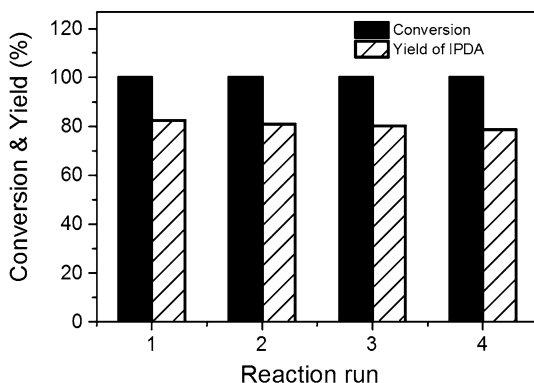
The Co/AC catalyst reduced by H₂ was also conducted. Results shows that the yield of IPDA is very low at loading of 5 wt% and 10 wt%, whilst increases dramatically and peaks at 67.4 mol% when the loading is 20 wt% (entry 3). By comparison, the Co/AC (N₂) is more preferable as it obtained 14.3 mol% higher in IPDA yield than that of Co/AC (H₂) at the same reaction conditions.

For concise, only the recyclability of 20 wt% Co/AC (N₂) was investigated, as depicted in Fig. 1. The conversion of IPN substantially maintains unchanged and the yield only shows marginal decline after four-time reused. The slight decline may be ascribed to the negligible loss of the active metal during the recycle process, showing that the catalyst is very stable for the hydroamination of IPN.

Catalyst characterization

Physical characterizations have been conducted in order to disclose the reason why Co/AC (N₂) showed superior catalytic performance to Co/AC (H₂). The XRD patterns of Co/AC heat-treated in N₂ are presented in Fig. 2. The peak at $2\theta = 26.6^\circ$ is assigned to C (002) crystal plane of graphite carbon (PDF#26-1079). The three diffraction peaks at $2\theta = 36.5^\circ$, 42.4° and 61.6° in each pattern correspond to CoO (111), (200), and (220) crystal planes (PDF#48-1719). Besides, the three diffraction peaks at $2\theta = 44.2^\circ$, 51.5° and 75.9° belong to face-centered cubic (fcc) Co (111), (200) and (220) (PDF#15-0806) [30, 31] and the diffraction peaks at $2\theta = 41.59^\circ$ and 47.39° are ascribed to hexagonal close-packed (hcp) Co (100) and (101) (PDF#05-0727) [31, 32]. It can be seen from Fig. 2a that Co species exist in the state of Co(II) and almost no atomic Co is detected while heat-treated at 300 °C or 400 °C in N₂. In contrast, almost all the Co species turns into metallic Co while heat-treated at 500 °C and 600 °C, indicating that Co ions in Co/AC precursor can be reduced into metallic Co by carbon during the heat-treatment over N₂, which is also demonstrated by our previous work [33] as well as other publications [34–36]. It is well known that Co generally

Fig. 1 Recyclability of 20 wt% Co/AC catalyst for IPN hydroamination. Reaction conditions: IPN, 2.5 g; methanol, 40 mL; NH₃ pressure, 0.2 MPa; H₂ pressure, 8 MPa; catalyst, 1.3 g; temperature, 80 °C; reaction time, 8 h; stirring speed, 1500 rpm



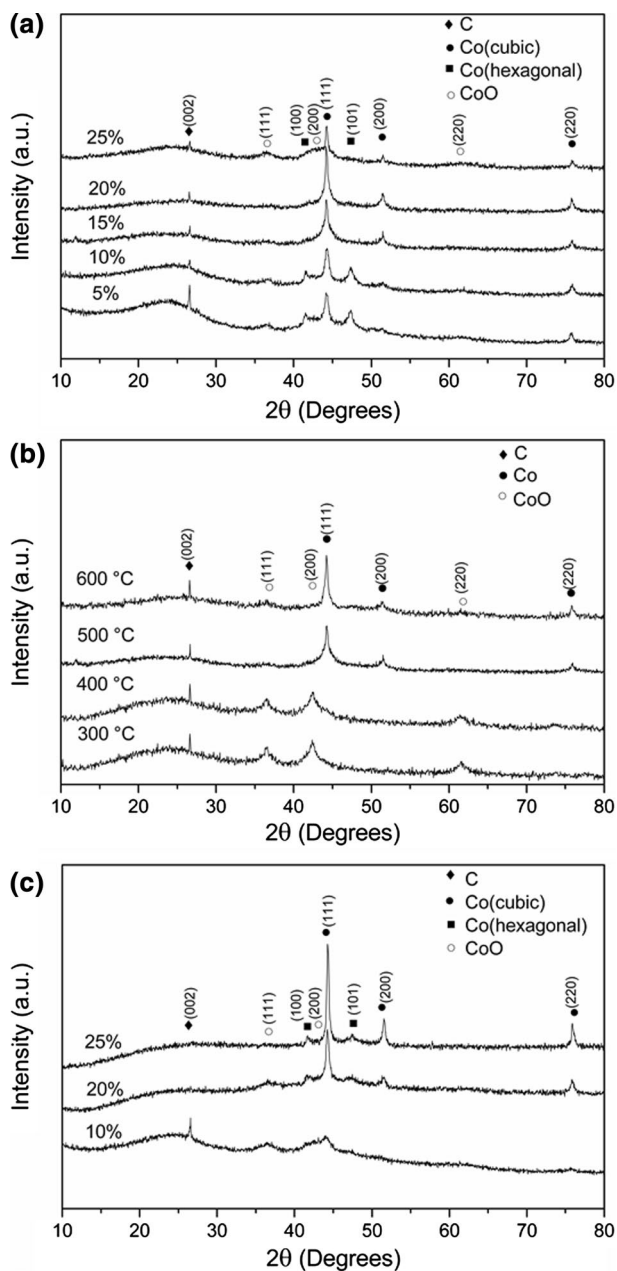


Fig. 2 XRD patterns of Co/AC: **a** Co/AC (N_2) catalyst heat-treated at different temperature, **b** Co/AC (N_2) catalysts with different Co loading and **c** Co/AC (H_2) catalysts with different Co loading

shows hydrogenation activity at its metallic state. This should be the reason why the Co/AC (N_2) heat-treated at 300 °C or 400 °C only obtained poor IPDA yield (Table S1). Moreover, the diffraction peak of Co (111) crystal plane for Co/AC heat-treated at 600 °C is narrower and sharper than that for Co/AC heat-treated at 500 °C. This implies that larger particle size of metallic Co is formed at 600 °C, which decreases the metal dispersion and the catalytic activity accordingly. This is also in agreement with the hydroamination reaction data that 500 °C is the optimal heat-treatment temperature.

Fig. 2b presents the XRD patterns at different loading of Co. Co in all five catalyst precursors are reduced to metallic Co after heat-treatment in N_2 at 500 °C. Significantly, the crystal form of Co in 5 wt% and 10 wt% Co/AC exist in the mixture forms of Co (hcp) and Co (fcc), while only Co (fcc) form exists in 15 wt%, 20 wt% and 25 wt% Co/AC. As reported [10], Co (fcc) crystal exhibits preferable catalytic activity comparing with Co (hcp). Consequently, 5 wt% and 10 wt% Co/AC shows inferior catalytic performance. Besides, the lower loading of Co generally leads to smaller particle size of the nano-metals, which is much easier to be oxidized during the reservation and therefore exhibits poor hydroamination activity [35].

The XRD patterns of Co/AC (H_2) are also depicted in Fig. 2c. Different from the Co/AC (N_2) catalysts, all the Co/AC (H_2) catalysts contain the mixture of fcc and hcp crystal forms of Co, indicating that the reduction condition would affect the crystal form much [37]. As a consequence, Co/AC (N_2) exhibit superior catalytic activity to Co/AC (H_2) since the hcp form of Co is less active in hydroamination reactions. Moreover, the particle sizes of Co metal calculated by the Scherrer equation [based on Co (111)] show that the 25 wt% and 20 wt% Co/AC (H_2) are about 25.4 nm and 20.7 nm, respectively, which are slightly larger than 19.8 nm and 17.7 nm for the corresponding particle sizes in the Co/AC (N_2) catalysts. The smaller particle size of Co in Co/AC (N_2) also supports its better catalytic performance.

Fig. 3 displays the TEM images of 20 wt% Co/AC heat-treated at 500 °C in N_2 and H_2 . Results show that the averaged particles sizes of these two catalysts are 11.6 nm and 17.8 nm. Although the sizes are varied from the XRD calculations, they have the same trend and also indicate the better activity of the former catalyst. The space of the lattice fringe for the Co/AC (N_2) is measured as 0.205 nm and 0.170 nm through Fourier transformation (Fig. 3b), in accordance with the fcc Co (111) and fcc Co (200), respectively [38]. By contrast, the space of the lattice fringe for the Co/AC (H_2) is measured as 0.204 nm and 0.198 nm (Fig. 3d), in accordance with the fcc Co (111) and hcp Co (111), respectively [38]. The results are in good agreement with the XRD analysis.

Fig. 4 presents the Co $2p_{3/2}$ and Co $2p_{1/2}$ spin-orbit components of 20 wt% Co/AC (N_2) heat-treated at 500 °C by XPS. The doublet peaks at the binding energy (BE) of 778.2 eV and 793.6 eV are attributed to Co^0 $2p_{3/2}$ and $2p_{1/2}$, indicating that Co can be reduced to metallic state after heat-treated at 500 °C in N_2 [39, 40], which is in accordance with our XRD analysis. Actually, oxidized Co is also observed, as evidenced by the existence of the doublet peaks at the binding energy (BE) of 780.2 eV and 795.6 eV, which belong to CoO $2p_{3/2}$ and $2p_{1/2}$, respectively [32, 41, 42]. This may be ascribed to the incomplete reduction or the re-oxidation of Co during the reservation of the catalyst.

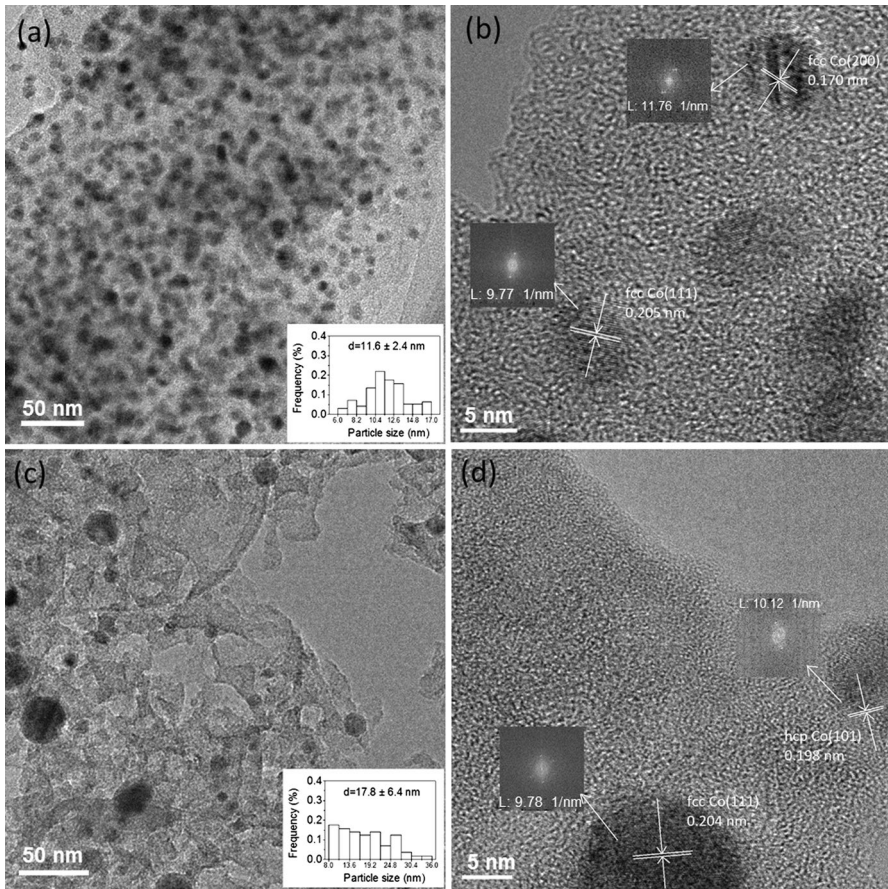


Fig. 3 TEM images: **a** and **b** 20 wt% Co/AC (N₂) catalysts heat-treated at 500 °C, **c** and **d** 20 wt% Co/AC (H₂) catalysts reduced at 500 °C

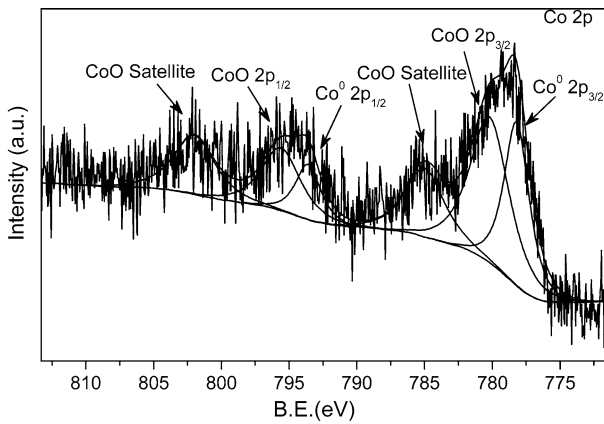


Fig. 4 Decomposed Co 2p XPS spectrum of 20 wt% Co/AC (N₂) catalysts

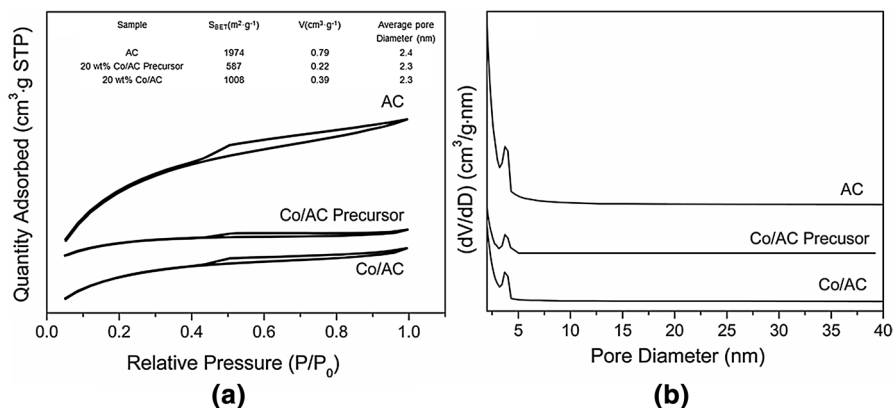


Fig. 5 BET characterization of 20 wt% Co/AC (N_2) catalysts: **a** nitrogen adsorption–desorption isotherms and **b** pore size distribution curves of the samples

The nitrogen sorption isotherms and pore-size distribution curves of the support and the Co catalysts with or without heat-treatment at 500 °C in N_2 are depicted in Fig. 5. All the three materials display typical type IV isotherm, indicating the existence of mesopores in the used commercially available AC [43, 44]. It can also be supported by the BJH pore diameter distribution derived from the desorption data with the average pore size of about 2.3 nm (Fig. 5b). From the inset table in Fig. 5a, one can see the same trend between the specific surface area and the pore volume of samples: it decrease first after impregnation of the metal precursor and then increase after heat-treatment. This could be ascribed that $\text{Co}(\text{NO}_3)_2$ comes inside and blocks the pores in the Co/AC precursor [27, 32], and part of carbon is consumed so that the specific surface area and pore volume are enlarged through the catalyst reduction in the followed heat-treatment process [35, 45], which might be beneficial for the mass diffusion during the hydroamination process. However, the specific surface area and pore volume of Co/AC are still smaller than those of AC. This is reasonable, as 20 wt% of Co residues in the mesopores. In addition, the particle size of Co is larger than 10 nm in terms of XRD and TEM analysis while BET shows the average pore diameter of AC is merely 2.3 nm, implicating that Co particles mainly distribute on the exterior surface of the AC support.

Conclusions

Supported Co/AC catalysts were prepared by the incipient wetness impregnation and the followed heat-treatment in N_2 and H_2 atmosphere, which were applied to the one-pot hydroamination of isophorone nitrile into isophorone diamine. The effect of heat-treatment temperature, metal loading and catalyst dosage was investigated. Results showed that the 20 wt% Co/AC (N_2) exhibited superior catalytic performance to the 20 wt% Co/AC (H_2), by which a maximum 90.2% yield of IPDA was achieved and it could be recycled at least four times. XRD, XPS, TEM and BET has

demonstrated that Co/AC precursor can be reduced into metallic Co by carbon during the heat-treatment over N₂ and the specific surface area and pore volume are also enlarged during that process. Meanwhile, the existence of fcc form of Co as well as the smaller and more uniformly dispersed Co particles in the Co/AC catalyst heat-treated in N₂ may contribute to the excellent catalytic performance.

Acknowledgements This research was supported by the National Natural Science Foundation of China (21878269 and 21476211) and the Natural Science Foundation of Zhejiang province (LY16B060004 and LY18B060016).

References

1. Fraga F, Vázquez I, Rodríguez-Núñez E, Martínez-Ageitos JM, Miragaya J (2009) Influence of the filler CaCO₃ on the cure kinetic of the epoxy network diglycidyl ether of bisphenol a (BADGE n=0) with isophorone diamine. *J Appl Polym Sci* 114:3338–3342
2. Ambrogio V, Brostow W, Carfagna C, Pannico M, Persico P (2012) Plasticizer migration from cross-linked flexible PVC: Effects on tribology and hardness. *Polym Eng Sci* 52:211–217
3. Liu Y, Sun K, Ma H, Xu X, Wang X (2010) Cr, Zr-incorporated hydrotalcites and their application in the synthesis of isophorone. *Catal Commun* 11:880–883
4. Sardon H, Irusta L, Fernández-Berridi MJ, Luna J, Lansalot M, Bourgeat-Lami E (2011) Waterborne polyurethane dispersions obtained by the acetone process: A study of colloidal features. *J Appl Polym Sci* 120:2054–2062
5. Schwarz M, Merkel A, Nitz JJ, Grund G (2014), Process for preparing 3-cyano-3,5,5-trimethylcyclohexanone. WO. 2012171830
6. Lettmann C, Streukens G, Orschel M, Grund G (2014), Process for preparing 3-aminomethyl-3,5,5-trimethylcyclohexylamine. US Patent 8,877,976
7. Ernst M, Hill T, Makarczyk P, Melder JP (2008) Continuous process for the hydrogenation of 3-cyano-3, 5, 5-trimethyl-cyclohexylimine. WO. 2008077852
8. Sánchez MA, Mazzieri VA, Sad MR, Grau R, Pieck CL (2011) Influence of preparation method and boron addition on the metal function properties of Ru Sn catalysts for selective carbonyl hydrogenation. *J Chem Technol Biotechnol* 86:447–453
9. Wang L, Wei Z, Liu Y (2013) Analysis of hydroamination products of isophoronenitrile by GC-MS. *Petrochem Technol* 42:563–567
10. Fischer A, Maciejewski M, Bürgi T, Mallat T, Baiker A (1999) Cobalt-catalyzed amination of 1,3-propanediol: effects of catalyst promotion and use of supercritical ammonia as solvent and reactant. *J Catal* 183:373–383
11. Louis K, Beauchene E, Vivier L, Dubois JL, Vigier KDO, Pouilloux PY (2016) Reductive amination of aldehyde ester from vegetable oils to produce amino ester in the presence of anhydrous ammonia. *ChemistrySelect* 1:2004–2008
12. Gomez S, Peters JA, Maschmeyer T (2002) The reductive amination of aldehydes and ketones and the hydrogenation of nitriles: mechanistic aspects and selectivity control. *Adv Synth Catal* 344:1037–1057
13. Krupka J, Pasek J (2012) Nitrile hydrogenation on solid catalysts—new insights into the reaction mechanism. *Curr Org Chem* 16:988–1004
14. Chatterjee M, Ishizaka T, Kawanami H (2016) Reductive amination of furfural to furfurylamine using aqueous ammonia solution and molecular hydrogen: an environmentally friendly approach. *Green Chem* 18:487–496
15. Schafer C, Nisanci B, Bere MP, Dastan A, Torok B (2016) Heterogeneous catalytic reductive amination of carbonyl compounds with Ni-Al alloy in water as solvent and hydrogen source. *Synthesis* 48:3127–3133
16. Segobia DJ, Trasarti AF, Apesteguia CR (2014) Conversion of butyronitrile to butylamines on noble metals: effect of the solvent on catalyst activity and selectivity. *Catal Sci Technol* 4:4075–4083

17. McAllister MI, Boulho C, McMillan L, Gilpin LF, Wiedbrauk S, Brennan C, Lennon D (2018) The production of tyramine via the selective hydrogenation of 4-hydroxybenzyl cyanide over a carbon-supported palladium catalyst. *RSC Adv* 8:29392–29399
18. Liu Y, Zhou K, Lu M, Wang L, Wei Z (2015) Synthesis of isophorone diamine and optimization of the reaction conditions. *J Chem Eng Chin Univ* 29:616–620 (**Chinese**)
19. Liu Y, Zhou K, Lu M, Wang L, Wei Z, Li X (2015) Acidic/basic oxides-supported cobalt catalysts for one-pot synthesis of isophorone diamine from hydroamination of isophorone nitrile. *Ind Eng Chem Res* 54:9124–9132
20. Birkenstock U, Holm R, Reinfandt B, Storp S (1985) Surface analysis of Raney catalysts. *J Catal* 93:55–67
21. Cerino PJ, Fleche G, Gallezot P, Salome JP (1991) Activity and stability of promoted Raney-nickel catalysts in glucose hydrogenation. *Stud Surf Sci Catal* 59:231–236
22. Liu Y, Yang X, Liu H, Ye Y, Wei Z (2017) Nitrogen-doped mesoporous carbon supported Pt nanoparticles as a highly efficient catalyst for decarboxylation of saturated and unsaturated fatty acids to alkanes. *Appl Catal B* 218:679–689
23. Wei Z, Lou J, Su C, Guo D, Liu H, Deng S (2017) An efficient and reusable embedded Ru catalyst for the hydrogenolysis of levulinic acid to γ -valerolactone. *Chemsuschem* 10:1720–1732
24. Zhang J, Wang L, Ji Y, Chen F, Xiao F (2018) Mesoporous zeolites for biofuel upgrading and glycerol conversion. *Front Chem Sci Eng* 12:132–144
25. Tang B, Dai W, Sun X, Wu G, Guan N, Hunger M, Li L (2015) Mesoporous Zr-Beta zeolites prepared by a post-synthetic strategy as a robust Lewis acid catalyst for the ring-opening aminolysis of epoxides. *Green Chem* 17:1744–1755
26. Komanoya T, Kinemura T, Kita Y, Kamata K, Hara M (2017) Electronic effect of ruthenium nanoparticles on efficient reductive amination of carbonyl compounds. *J Am Chem Soc* 139:11493–11499
27. Yang Y, Jia L, Hou B, Li D, Wang J, Sun Y (2014) The correlation of interfacial interaction and catalytic performance of N-doped mesoporous carbon supported cobalt nanoparticles for Fischer-Tropsch synthesis. *J Phys Chem C* 118:268–277
28. Dong B, Guo X, Zhang B, Chen X, Guan J, Qi Y, Han S, Mu X (2015) Heterogeneous Ru-based catalysts for one-pot synthesis of primary amines from aldehydes and ammonia. *Catalysts* 5:2258–2270
29. Liu Y, Zhou K, Shu H, Liu H, Lou J, Guo D, Wei Z, Li X (2017) Switchable synthesis of furfurylamine and tetrahydrofurfurylamine from furfuryl alcohol over RANEY® nickel. *Catal Sci Technol* 7:4129–4135
30. Fu T, Jiang Y, Lv J, Li Z (2013) Effect of carbon support on Fischer-Tropsch synthesis activity and product distribution over Co-based catalysts. *Fuel Process Technol* 110:141–149
31. Wang T, Ding Y, Lue Y, Zhu H, Lin L (2008) Influence of lanthanum on the performance of Zr-Co/activated carbon catalysts in Fischer-Tropsch synthesis. *J Nat Gas Chem* 17:153–158
32. Du H, Zhu H, Zhao Z, Dong W, Luo W, Lu W, Jiang M, Liu T, Ding Y (2016) Effects of impregnation strategy on structure and performance of bimetallic CoFe/AC catalysts for higher alcohols synthesis from syngas. *Appl Catal A* 523:263–271
33. Wei Z, Lou J, Su C, Guo D, Liu Y, Deng S (2017) An efficient and reusable embedded Ru catalyst for the hydrogenolysis of levulinic acid to γ -valerolactone. *Chemsuschem* 10:1720–1732
34. Xiong H, Motchelaho MAM, Moyo M, Jewell LL, Coville NJ (2011) Correlating the preparation and performance of cobalt catalysts supported on carbon nanotubes and carbon spheres in the Fischer-Tropsch synthesis. *J Catal* 278:26–40
35. Zhu Z, Lu M, Zhuang Y, Shen D (1999) A comparative study of N₂O conversion to N₂ over Co/AC and Cu/AC catalysts. *Energy Fuels* 13:763–772
36. Lv J, Huang C, Bai S, Jiang Y, Li Z (2012) Thermal decomposition and cobalt species transformation of carbon nanotubes supported cobalt catalyst for Fischer-Tropsch synthesis. *J Nat Gas Chem* 21:37–42
37. Xiong H, Moyo M, Rayner MK, Jewell LL, Billing DG, Coville NJ (2010) Autoreduction and catalytic performance of a cobalt Fischer-Tropsch synthesis catalyst supported on nitrogen-doped carbon spheres. *ChemCatChem* 2:514–518
38. Dong W, Liu J, Zhu H, Ding Y, Pei Y, Liu J, Du H, Jiang M, Liu T, Su H, Li W (2014) Co-Co₂C and Co-Co₂C/AC catalysts for hydroformylation of 1-hexene under low pressure: experimental and theoretical studies. *J Phys Chem C* 118:19114–19122
39. Xue J, Cui F, Huang Z, Zuo J, Chen J, Xia C (2011) Liquid phase hydrogenolysis of biomass-derived lactate to 1,2-propanediol over silica supported cobalt nanocatalyst. *Chin J Chem* 29:1319–1325

40. Morales F, Groot FMFD, Gijzeman OLJ, Mens A, Stephan O, Weckhuysen BM (2005) Mn promotion effects in Co/TiO₂ Fischer-Tropsch catalysts as investigated by XPS and STEM-EELS. *J Catal* 230:301–308
41. Chen P, Yang F, Kostka A, Xia W (2014) Interaction of cobalt nanoparticles with oxygen- and nitrogen-functionalized carbon nanotubes and impact on nitrobenzene hydrogenation catalysis. *ACS Catal* 4:1627–1636
42. Jalama K (2016) Fischer-Tropsch synthesis over Co/TiO₂ catalyst: effect of catalyst activation by CO compared to H₂. *Catal Commun* 74:71–74
43. Qian W, Zhang H, Ying W, Fang D (2011) Product distributions of Fischer-Tropsch synthesis over Co/AC catalyst. *J Nat Gas Chem* 20:389–396
44. Malobela LJ, Heveling J, Augustyn WG, Cele LM (2014) Nickel-cobalt on carbonaceous supports for the selective catalytic hydrogenation of cinnamaldehyde. *Ind Eng Chem Res* 53:13910–13919
45. Bekyarova E, Mehandjiev D (1993) Effect of calcination on Co-impregnated activated carbon. *J Colloid Interface Sci* 161:115–119

Publisher's Note Springer Nature remains neutral with regard to jurisdictional claims in published maps and institutional affiliations.